Periodic Anderson Model in Infinite Dimensions

M. Jarrell and Hossein Akhlaghpour
Department of Physics, University of Cincinnati, Cincinnati, Ohio 45221

Th. Pruschke
Institut für Theoretische Physik, Universität Regensburg, Universitätsstrasse 31, W-8400 Regensburg, Germany
(Received 21 September 1992)

The symmetric periodic Anderson model is studied in the limit of infinite spatial dimensions within an essentially exact quantum Monte Carlo method. The single-particle spectral function develops a gap Δ, and the neutron structure factor also develops a gap $\approx 2\Delta$. Depending upon the ratio of Δ to other energy scales, there is a transition to an antiferromagnetic state. In the paramagnetic state, both the f orbital specific heat and ferromagnetic susceptibility display rough scaling with T/Δ; for $T > \Delta$ they are heavy-fermion-like while for $T < \Delta$ they are insulatorlike.

PACS numbers: 71.30.+h, 65.50.+m, 71.28.+d, 75.20.Hr

Since the discovery of the heavy-fermion materials with rare-earth or actinide elements [1] the periodic Anderson model (PAM) was considered the most promising candidate to at least qualitatively describe the rich physics in these materials. From early studies it is known that most of the unusual properties of these materials like the large coefficient in the specific heat, transport properties, and even magnetic and superconducting properties can be qualitatively accounted for [1]. Quantitative agreement with experiments is sometimes possible due to the fact that over a large region these systems may be regarded as a regular array of *independent* Kondo scatterers, which makes it possible to calculate especially thermodynamic quantities using the extremely well understood impurity Anderson model [1,2].

However, in view of the controversial two-particle properties of these materials it is desirable to have an exact solution of the *periodic* Anderson model in a nontrivial limit. A quite general limit to obtain sensible approximate or even exact results for such *locally* highly correlated models is the limit of infinite dimensions [3–5]. In this limit the dynamics of the system become essentially local [4] which considerably simplifies the task of calculating physical quantities [5]. Recently, several groups independently proposed a mean-field theory for the Hubbard model based on the special properties in this limit [6–9] and were able to calculate a variety of quantities approximately [8] or even essentially exactly [9,10]. In this Letter we demonstrate that this procedure can be extended to the periodic Anderson model. In combination with exact quantum Monte Carlo (QMC) procedures [11] we calculate one- and two-particle properties of this model which can be viewed as essentially *exact* results for the periodic Anderson model in a nontrivial limit.

Although the inclusion of more realistic features presents no fundamental difficulty for our method, we want to concentrate on the simplest version of the periodic Anderson model

$$H=\sum_{\mathbf{k}\sigma}\epsilon_{\mathbf{k}}d^{\dagger}_{\mathbf{k}\sigma}d_{\mathbf{k}\sigma}+\sum_{\nu\sigma}(\epsilon_d d^{\dagger}_{\nu\sigma}d_{\nu\sigma}+\epsilon_f f^{\dagger}_{\nu\sigma}f_{\nu\sigma}) +\sum_{\nu}U(n_{f\nu\uparrow}-\tfrac{1}{2})(n_{f\nu\downarrow}-\tfrac{1}{2}) +V\sum_{\mathbf{k}\sigma}(d^{\dagger}_{\mathbf{k}\sigma}f_{\mathbf{k}\sigma}+\text{H.c.})\,. \tag{1}$$

In (1), $d(f)^{(\dagger)}_m$ destroys (creates) a d (f) electron with quantum numbers $\{\mathbf{k}(\nu),\sigma\}$, $\epsilon_{\mathbf{k}}$ denotes the dispersion for the extended d states, U is the screened Coulomb matrix element for the localized f states, and V characterizes the mixing between the two subsystems.

Although the lattice structure is not essential to our arguments, we will study the model (1) on a simple hypercubic lattice of dimension D and assume that the dominant contributions to the dispersion $\epsilon_{\mathbf{k}\sigma}$ come from transfer matrix elements along the coordinate axes to the first (t_1) and second (t_2) neighbors in each direction. Although this surely is an oversimplifying assumption for real systems, it has the advantage that the free density of states (DOS) in the limit $D\rightarrow\infty$ becomes purely Gaussian, $A^{d0}(\epsilon)=\exp\{-(\epsilon/\epsilon^*)^2\}/(\pi\epsilon^{*2})^{1/2}$, with a width such that $\epsilon^{*2}\equiv 2\langle\epsilon^2_{\mathbf{k}\sigma}\rangle_{\mathbf{k}}$ [5]. We choose $\epsilon^*=1$ as a convenient energy scale for the remainder of this Letter.

Since dynamics become essentially local for $D=\infty$ [3,4], one can use the fact that the proper one-particle self-energy is then $\mathbf{k}$ independent to resum the perturbation series and obtain an effective impurity Anderson model with a self-consistently determined medium [6–9]. For the Hamiltonian (1), these equations read [12]

$$G^f_{\nu\nu,\sigma}(z)=\int d\epsilon\,\rho_d^{(0)}(\epsilon)[z-\epsilon_f-\Sigma_\sigma(z) -V^2(z-\epsilon_d-\epsilon)^{-1}]^{-1}\,, \tag{2}$$

$$\tilde{\Delta}(z)=\mathrm{Im}\{[G^f_{\nu\nu,\sigma}(z)]^{-1}+\Sigma_\sigma(z)\}|_{z=\omega+i0^+}\,, \tag{3}$$

where $G^f_{\mu\nu,\sigma}(z)$ denotes the one-particle Green's function for the f states and $\tilde{\Delta}(z)$ is the effective mixing due to the

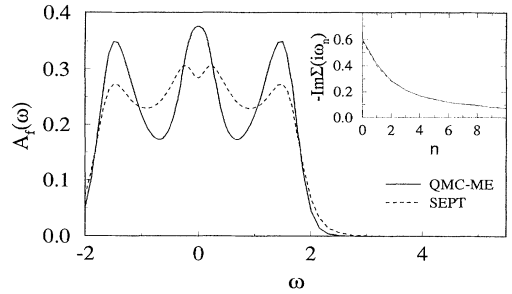

FIG. 1. The f-electron DOS obtained from QMC and maximum-entropy method (QMC-ME), and that obtained from perturbation theory (SEPT) when $U=2.0$, $V=0.5$, $\epsilon_d=\epsilon_f=0$, and $T=0.2$. The corresponding imaginary frequency self-energies are shown in the inset.

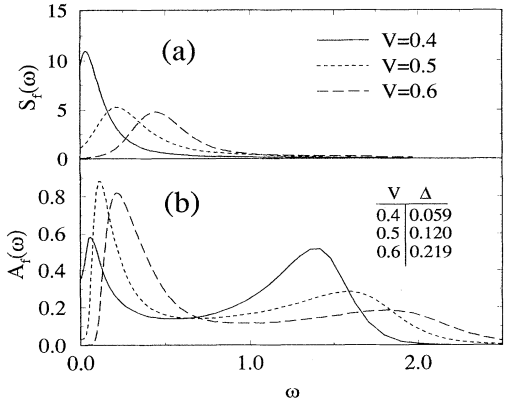

FIG. 2. (a) Local neutron structure factor $S_f(\omega)$ and (b) f-electron single-particle density of states $A_f(\omega)$ when $U=2.0$, $T=0.05$, and $\epsilon_f=\epsilon_d=0$ for various values of V.

bare mixing V and the presence of all other f states at sites other than v. Obviously, Eqs. (2) and (3) form a closed self-consistency cycle to determine $\Sigma(z)$. The difficulty remains that, in order to obtain a refined $\Sigma(z)$ from an initial guess, one has to solve the impurity Anderson model defined by (3). Among the several different methods to tackle this problem, QMC is the most efficient for the current purposes, since it (i) is essentially exact and (ii) allows us to address two-particle properties in addition to the one-particle spectra [9].

Recently, a renewed interest has occurred in a special class of lanthanide-based compounds such as CeNiSn [13] or $Ce_3Bi_4Pt_3$ [14,15], which show a behavior reminiscent of normal heavy-fermion materials at high temperatures but become insulating, i.e., develop a gap, at low temperatures. In these materials the f-electron contribution to experimental measurements is isolated by taking the difference of measurements on the Ce compound and the isostructural La analog [13–15]. That the periodic Anderson model in the symmetric limit, $\epsilon_f=\epsilon_d=0$, may indeed provide a (pseudo)gap in the one-particle excitation spectrum is well known [16,17]. It is therefore interesting to study its relevance for these materials, and, in the interest of brevity, we will limit our discussion to the symmetric case.

The maximum-entropy (ME) method was used to obtain real-frequency results, $S_f(\omega)$ and $A_f(\omega)$, from imaginary time QMC data [18]. $S_f(\omega)$ is the f-electron neutron structure factor $S_f(\mathbf{q},\omega)$ integrated over all $\mathbf{q}$. It was obtained using the method described in Ref. [19]. $A_f(\omega)=-(1/\pi)\mathrm{Im}G^f_{vv}(\omega+i0^+)$ is the f-electron density of states. Here, second-order site-excluded perturbation theory (SEPT) in U, in which the self-energy was subtracted off from the site propagator during the self-consistency step [8], was used to produce a default model for the maximum entropy process. The SEPT method represents a good starting point for the analytic continuation which then uses the QMC result to obtain more precise information. As shown in the inset to Fig. 1, the agreement between the imaginary time QMC and SEPT results is good. However, there was always a statistically significant difference between the QMC and SEPT results. These small differences in the imaginary time results yield larger differences in the real frequency results (Fig. 1). The differences between SEPT and QMC-ME become greater when U/V^2 or T increases, and are extremely important when calculating dynamic quantities such as transport [20]. Thus, all subsequent dynamical information reported here was obtained with the ME method.

In Fig. 2, $A_f(\omega)$ and $S_f(\omega)$ are plotted for various values of V when $T=0.05$ and $U=2.0$. These values of U and V are sufficient to ensure that the results are in the strongly correlated regime, for which $\langle(n_\uparrow-n_\downarrow)^2\rangle>0.75$. Both $A_f(\omega)$ and $S_f(\omega)$ display a gap [when $V=0.4$, a gap forms in $S(\omega)$ at still lower temperatures]. The d and total DOS (not shown) also display a gap of roughly the same size as the f DOS. However, the magnetic gap Δ_m is slightly larger than twice the single-particle gap Δ, when both are measured from $\omega=0$ to the frequency of the peak. A magnetic gap $\Delta_m\approx 2\Delta$ was recently found in $Ce_3Bi_4Pt_3$ [15], in which $\Delta\approx 5$ meV and $\Delta_m\approx 12$ meV. This is expected [15], since to lowest order in U the con-

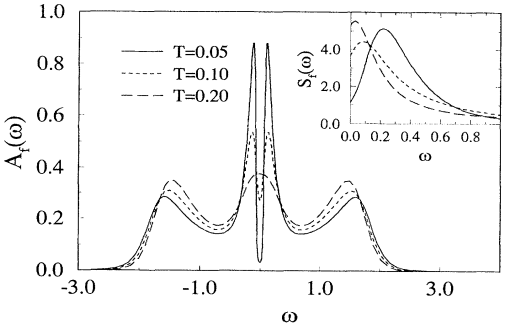

FIG. 3. Temperature dependence of $A_f(\omega)$ and $S_f(\omega)$ when $V=0.5$, $U=2.0$, and $\epsilon_f=\epsilon_d=0$.

tribution to the magnetic susceptibility is particle-hole excitations which need a minimum excitation energy of the order of the full single-particle gap 2Δ. The approximate values of Δ appear in the table inset in Fig. 2(b).

The temperature evolution of $A_f(\omega)$ and $S_f(\omega)$ is shown in Fig. 3. As the temperature is lowered, $A_f(\omega)$ first begins to develop a Kondo-like peak at the chemical potential. However, before the peak can become sharp, the gap begins to form when $T \approx \Delta$ [1]. The evolution of $S_f(\omega) = \chi''(\omega)/[1 - \exp(-\beta\omega)]$ is shown in the inset to Fig. 3. For high temperatures $S_f(\omega)$ is essentially identical to the impurity result [19]. As T is lowered, and after the single-particle gap begins to form, $S_f(\omega)$ begins to develop a gap $\Delta_m \approx 2\Delta$.

In Fig. 4 we show the f (d) renormalization factor $\zeta_{f(d)}^{-1}(T) = 1 - \mathrm{Im}\Sigma^{f(d)}(\omega_0)/\omega_0$, where $\omega_0 = \pi T$ and $\Sigma^{f(d)}$ is the total f (d) self-energy [21], and the contribution of the f states to the specific heat $\Delta\gamma_f(T) = \Delta C_f(T)/T$. The inset in Fig. 4(b) displays the total $\gamma(T) = C(T)/T$ when $V = 0.5$. Note that $\Delta\gamma_f$ and $\Delta\zeta_f^{-1}$ display a rough universal scaling with T/Δ, and that γ_f and γ have pronounced peaks at $T \approx \Delta$. The latter has been seen in CeNiSn [13]. At high T, where the system is a metal, both γ_f and $\zeta_f^{-1}(T)$ are approximate measures of the f-electron effective mass, and are roughly proportional. As the temperature is lowered, both first rise like in a usual heavy-fermion system. However, before the heavy-fermion state can form completely the gap begins to open and this rough proportionality is broken, indicating the formation of an insulating state. The occurrence of this insulating state is directly connected to the perfect particle-hole symmetry in the present case and has a rather intuitive physical reason: As $T \ll \Delta$, the Kondo effect leads to a scattering resonance at or near the chemical potential. Since there exists a level crossing between these dynamically generated local quasiparticle states and the conduction-band states, one will find a splitting with a gap at the position of the resonance [22]. For the particle-hole symmetry under consideration the resonance develops exactly at the chemical potential [16,17], i.e., the resulting system consequently is an insulator.

In Fig. 5, the f-orbital magnetic susceptibilities are plotted versus T/Δ. Consistent with what is seen in $Ce_3Bi_4Pt_3$ [14], the ferromagnetic susceptibility displays a broad peak when $T \approx \Delta$. $\Delta\chi_F$ and the screened local moment $T\chi_{ii}$ vs T/Δ fall onto a single curve for different values of V, indicating rough universality with Δ as the scale. The antiferromagnetic susceptibility χ_{AF} is quite nonuniversal. The $V = 0.4$ and $V = 0.5$ results display a transition with a small screened local moment $T\chi_{vv}$. Whereas the $V = 0.6$ result does not display a transition. The lack of universality of χ_{AF} is probably due to the fact that the intersite RKKY exchange mediated by the conduction band does not scale with Δ [23] (which probably also yields some slight variations of scaling of χ_F). Depending upon the relative size of Δ and the RKKY exchange, we get either a paramagnetic state or an antiferromagnetic transition.

In addition to depending upon U and V, the antiferromagnetic transition in the symmetric model is quite sensitive to nesting. To demonstrate this, we added a second hopping term t_2 to the second neighbor along the axial direction, which acts to frustrate the Néel order. As shown in the inset to Fig. 5(b) the Néel transition temperature T_N is quickly depressed when t_2/t_1 becomes finite. Furthermore, using the methods outlined by Müller-Hartmann [4], one may calculate the susceptibility $\chi(x)$ for different values of

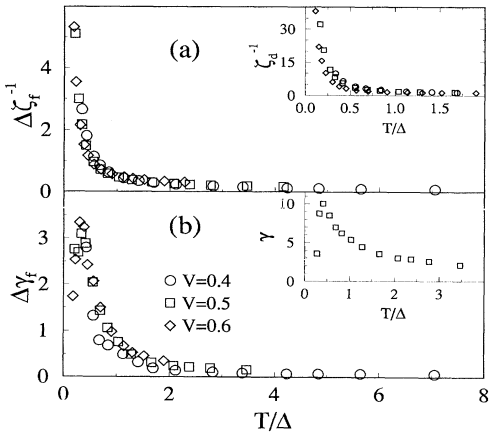

FIG. 4. (a) The f and d renormalization factors, and (b) the scaled f electron γ_f vs T/Δ when $U = 2.0$ and $\epsilon_d = \epsilon_f = 0$, for various V. In the inset to (b), the total γ is plotted vs T/Δ when $V = 0.5$.

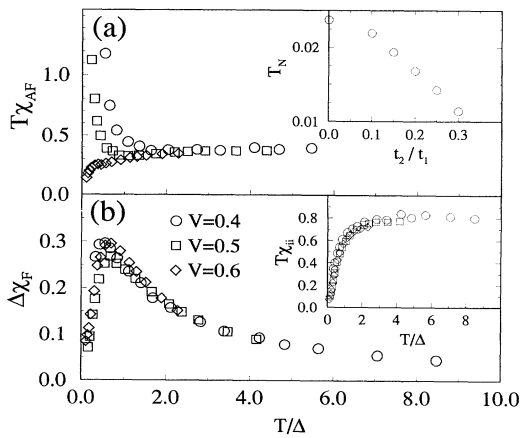

FIG. 5. Susceptibilities of the symmetric PAM when $U = 2.0$ for various values of V. The inset of (a) shows the Néel temperature T_N when $V = 0.4$ as a function of a frustrating hopping t_2/t_1.

$$x(\mathbf{q}) = \frac{1}{d(t_1^2+t_2^2)} \sum_l [t_1^2 \cos(q_l) + t_2^2 \cos(2q_l)] . \quad (4)$$

For the symmetric model in the paramagnetic state, we found that $\chi(x)$ rises monotonically as x falls from 1. However, for $t_2/t_1 > 0.5$, the smallest (most negative) value of x no longer occurs at the Néel point in the Brillouin zone $\mathbf{q} = (\pi,\pi,\pi,\ldots)$, rather it falls on a point on a hypersurface centered around the Néel point. Thus for $t_2/t_1 > 0.5$, any remaining transitions are to an incommensurate state.

In addition to discussing what we found in the PAM, it is useful to discuss what was not found. From a direct calculation of the RKKY exchange [23], one might conclude that ferromagnetism would be favored for the model very far away from half filling. However, we did not find a divergent ferromagnetic susceptibility for any filling or set of parameters. Perhaps screening of the local moments inhibits the transition. In addition, we found that s-wave symmetry superconductivity was always suppressed by the correlations.

In conclusion, we have provided an essentially exact solution of the infinite dimensional PAM. For brevity, we have concentrated on the symmetric limit, and show that the f spectrum, specific heat, electronic renormalization factors, and susceptibility are heavy-fermion-like for high T, and insulatorlike for low T. This, as well as the gap in $S_f(\omega)$ and the behavior of $\gamma = C/T$ are consistent with experiment. In addition, we have shown that $\Delta\chi_F$ and $\Delta\gamma_f$ scale with T/Δ. Our method may also be applied to the asymmetric limit, and used to obtain transport properties. These results along with a quantitative comparison to experimental data will be presented elsewhere [20,23].

We would like to acknowledge useful conversations with D. L. Cox, J. Freericks, R. Fye, B. Goodman, N. Grewe, D. Hess, M. Hundley, V. Janiš, Matthew Steiner, and F. C. Zhang. This work was supported by National Science Foundation Grant No. DMR-9107563, and by the Ohio Supercomputing Center.

[1] For a recent review, see N. Grewe and F. Steglich, in *Reports on Physics and Chemistry of Rare Earths* (North-Holland, Amsterdam, 1991), Vol. 14, p. 343.
[2] P. Schlottmann, Phys. Rep. **181**, 1 (1989).
[3] W. Metzner and D. Vollhardt, Phys. Rev. Lett. **62**, 324 (1989).
[4] E. Müller-Hartmann, Z. Phys. B **74**, 507 (1989).
[5] U. Brandt and Ch. Mielsch, Z. Phys. B **75**, 365 (1989); **79**, 295 (1990).
[6] F. J. Ohkawa, Prog. Theor. Phys. Suppl. **106**, 95 (1991).
[7] V. Janiš, Z. Phys. B **83**, 227 (1991); V. Janiš and D. Vollhardt, Int. J. Mod. Phys. B **6**, 731 (1992).
[8] A. Georges and G. Kotliar, Phys. Rev. B **45**, 6479 (1992).
[9] M. Jarrell, Phys. Rev. Lett. **69**, 168 (1992); Th. Pruschke, D. L. Cox, and M. Jarrell (to be published); M. Jarrell and Th. Pruschke, Z. Phys. B (to be published).
[10] M. Rosenberg, X. Zhang, and G. Kotliar, Phys. Rev. Lett. **69**, 1236 (1992); A. Georges and W. Krauth, *ibid.* **69**, 1240 (1992).
[11] J. E. Hirsch and R. M. Fye, Phys. Rev. Lett. **56**, 2521 (1986).
[12] A. Georges, G. Kotliar, and Q. Si, Int. J. Mod. Phys. B **6**, 705 (1992).
[13] T. Takabatake *et al.*, Phys. Rev. B **41**, 9607 (1990).
[14] M. F. Hundley *et al.*, Phys. Rev. B **42**, 6842 (1990).
[15] A. Severing *et al.*, Phys. Rev. B **44**, 6832 (1991).
[16] K. Yamada and K. Yoshida, in *Theory of Heavy Fermions and Valence Fluctuations*, edited by T. Kasuya and T. Saso (Springer, Berlin, 1985).
[17] Th. Pruschke and N. Grewe, Z. Phys. B **74**, 439 (1989).
[18] R. K. Bryan, Europhys. Biophys. J. **18**, 165 (1990); J. E. Gubernatis *et al.*, Phys. Rev. B **44**, 6011 (1991); R. N. Silver *et al.*, Phys. Rev. B **41**, 2380 (1989).
[19] M. Jarrell, J. E. Gubernatis, and R. N. Silver, Phys. Rev. B **44**, 5347 (1991).
[20] Th. Pruschke and M. Jarrell (to be published).
[21] J. W. Serene and D. W. Hess, Phys. Rev. B **44**, 3391 (1991); S. Yip, Phys. Rev. B **38**, 8785 (1988).
[22] N. Grewe, Solid State Commun. **50**, 19 (1984).
[23] M. Jarrell, Th. Pruschke, and H. Akhlaghpour (to be published).